INSTITUTE OF PHYSICS PUBLISHING PLASMA PHYSICS AND CONTROLLED FUSION

Plasma Phys. Control. Fusion **47** (2005) B195–B206 doi:10.1088/0741-3335/47/12B/S15

Heat and particle transport in a tokamak: advances in nonlinear gyrokinetics

F Jenko, T Dannert and C Angioni

Max-Planck-Institut für Plasmaphysik, EURATOM Association, 85748 Garching, Germany

Received 1 July 2005
Published 3 November 2005
Online at stacks.iop.org/PPCF/47/B195

Abstract

Nonlinear and quasilinear gyrokinetics are used in tandem to address two key open questions in the area of turbulent transport in magnetized fusion plasmas. These are, first, the qualitative and quantitative properties of electron thermal transport caused by trapped electron modes and, second, the existence and nature of an anomalous particle pinch. Both of these issues are examined in a multispecies, fully kinetic framework.

(Some figures in this article are in colour only in the electronic version)

1. Introduction

It is widely recognized in the fusion community that over the past 10–15 years, there has been considerable progress in characterizing, understanding and even controlling plasma microturbulence. On the theory side, this stride was greatly facilitated by the advent of large-scale supercomputers in the early to mid-1990s. However, until fairly recently, most core turbulence studies focused on transport induced by ion temperature gradient (ITG) modes in the so-called adiabatic electron limit. While this approximation greatly simplifies the numerical treatment (in particular by removing the time scale separation between the parallel electron motion and the remaining dynamics), it also causes the particle and electron heat fluxes to vanish identically. Thus, there is presently a large gap between our level of understanding of ion thermal transport and that of all remaining transport channels. This paper intends to be a contribution to the attempt to close this gap. We will use nonlinear and quasilinear gyrokinetics in tandem to address two key open questions: the qualitative and quantitative properties of electron thermal transport caused by trapped electron modes (TEMs) and the existence and nature of an anomalous particle pinch in ITG and TEM turbulence.

The rest of this paper is organized as follows. In section 2, the tools used for this study are introduced. These are, on the one hand, the nonlinear gyrokinetic continuum code `gene` and, on the other hand, a modified quasilinear transport model which is able to capture and predict several features of turbulent systems with reasonable accuracy. In section 3, these tools are applied to the problem of collisionless TEM turbulence. Here, we will be interested primarily

in the scaling of the electron heat flux with the normalized electron temperature gradient, R/L_{T_e}, shedding light on an issue which has been the focus of several experimental studies in recent years. In section 4, we will turn our attention to the particle transport induced by ITG and TEM turbulence. In this context, we will find that in both cases, the resulting net particle flux may be directed inwards (i.e. up-gradient) for small values of the normalized density gradient, R/L_n. Maybe surprisingly, both trapped *and passing* electrons may contribute to this particle pinch, an effect which can be explained by means of quasilinear theory. Section 5 contains a summary of the key physics results.

2. Numerical tools

2.1. Nonlinear gyrokinetics

The main tool used in this paper for the study of plasma microturbulence is the nonlinear gyrokinetic code `gene`. It solves the electromagnetic gyrokinetic equations [1, 2] in the field-line-following coordinates employing toroidal flux tubes. Both trapped and passing particles are retained. Although the code can handle arbitrary magnetic geometry, we restrict the magnetohydrodynamic equilibrium to the widely used $\hat{s}$-α model (with α set to zero) here. Using a so-called continuum approach, each particle species' distribution function is represented on a grid in phase space and time [3]. Recently, `gene` has been improved significantly with respect to various algorithmic features. It now employs fourth-order and sixth-order (compact) finite difference schemes as well as quasi-spectral methods in phase space, along with third-order Runge–Kutta time stepping.

`gene` has been benchmarked successfully in the linear regime. A subset of the equations (describing parallel electron motion) which is responsible for the dynamics of kinetic shear Alfvén waves was studied in [4]. It was shown that with a moderate number of velocity grid points, the algorithm reproduces the exact results from a corresponding dispersion relation with high precision. Moreover, `gene` results for the complex frequencies of ITG modes, TEMs and kinetic ballooning modes typically lie within a few per cent of the respective `gs2` [5] results (examples are shown in [6]). Another important linear test is the (partial) damping of axisymmetric modes of the electrostatic potential. Here, we retain both passing and trapped ions but assume the electrons to be adiabatic. According to the theory of Rosenbluth and Hinton, the time evolution of the potential amplitude may be described as the superposition of damped oscillations (the so-called geodesic acoustic modes) and a finite residuum [7, 8]. The latter is given by the formula

$$\lim_{t\to\infty} \frac{\phi}{\phi_0} = \frac{1}{1+1.6/h}, \tag{1}$$

where $h \equiv \epsilon^{1/2}/q^2$. As can be inferred from figure 1, there is good agreement between the analytic results and the `gene` simulations.

Nonlinear benchmarks, although necessary, are much harder to perform than linear ones. Presently, there is only one set of physical parameters for which a fairly large number of independent simulations agree. This is the so-called Cyclone base case: $R/L_{T_i} = 6.9$, $R/L_n = 2.2$, $q = 1.4$, $\hat{s} = 0.8$, $T_e/T_i = 1$, $\epsilon \equiv r/R = 0.18$. For simplicity, the flux surfaces are taken to be circular and concentric, and finite β effects and collisions are neglected. We obtain $\chi_i = 1.84\,\rho_s^2 c_s/a$ for adiabatic ITG turbulence (see figure 2) where ρ_s and c_s are, respectively, the thermal ion Larmor radius at electron temperature and the ion sound speed. This number is in good agreement with the results by Dimits ($\chi_i = 1.90\rho_s^2 c_s/a$), Candy and Waltz ($\chi_i = 1.85\rho_s^2 c_s/a$) and Dorland ($\chi_i = 1.86\rho_s^2 c_s/a$) [9].

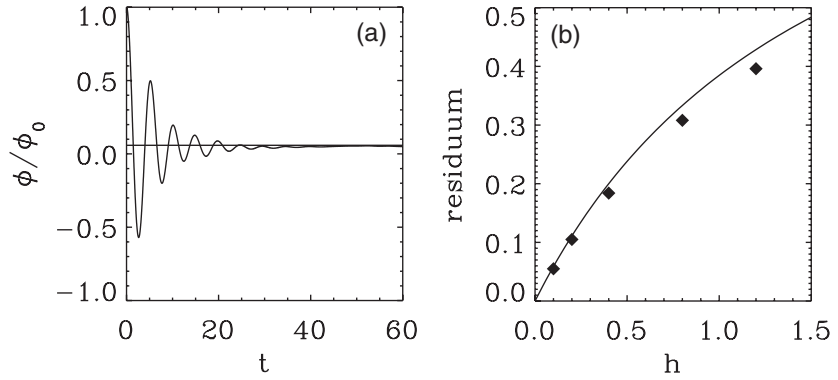

Figure 1. Test case: linear damping of zonal (i.e. only radially varying) potentials. (*a*) Typical time trace of ϕ/ϕ_0. (*b*) The long-time residuum as a function of the parameter $h \equiv \epsilon^{1/2}/q^2$. Simulation results are shown as diamonds while the solid line indicates the theoretical prediction by Rosenbluth and Hinton.

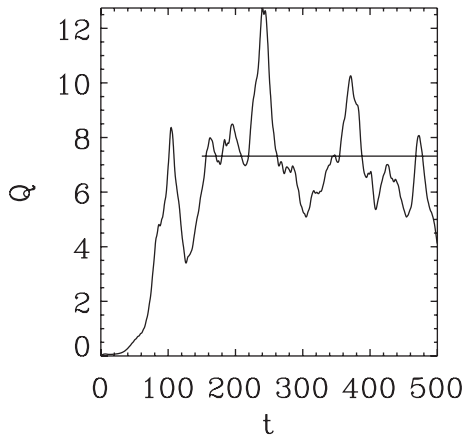

Figure 2. Test case: time trace of turbulent ion heat flux Q for Cyclone base case parameters in units of $(\rho_s^2 c_s/L_n)(p_i/L_n)$. The straight solid line indicates the mean value between $t = 150$ and $t = 500$ where the time unit is L_n/c_s.

2.2. A modified quasilinear transport model

Recent numerical experiments with gene revealed that the transport-dominating modes in a nonlinear simulation sometimes resemble the respective linear modes to a remarkable degree [10]. In particular, when Fourier transforming pairs of fluctuating quantities in the periodic y direction and plotting the probability density function (PDF) of their cross phases as a function of k_y, one finds that in the long-wavelength regime, i.e. for $k_y\rho_s \sim 0.1$–0.15, these PDFs exhibit clear peaks about the value of the linear cross phase. This scale range is also the one in which the k_y spectra of the cross-field turbulent fluxes generally peak. In contrast the PDFs tend to show little structure at shorter wavelengths, i.e. for $k_y\rho_s \gtrsim 0.3$. This means that the cross phases are more or less random at small scales (see also [3]). This finding implies that one should be able to link the easily accessible information on linear cross phase relations to the properties of turbulent transport, provided one focuses on the relevant length scales. In the literature, one finds numerous quasilinear studies which highlight the

role of smaller perpendicular scales, $k_y\rho_s \sim 0.3$–0.5, corresponding roughly to the position of the maximum linear growth rate. We will see below that this can be misleading. On the other hand, this 'standard approach' can be generalized in a straightforward way, provided one addresses the nontrivial problem of finding a reasonably simple way to estimate the relevant k_y range.

In [10], the following approach has been proposed. It is based on linear gyrokinetic simulations with the gs2 code [5]. As a reasonable starting point we take the heuristic mixing length estimate

$$\chi_e \sim D \sim \gamma/k_\perp^2. \tag{2}$$

We note that for a given k_y, the fastest growing toroidal (i.e. curvature-driven) microinstabilities tend to be those with $k_x = 0$. This corresponds to radially elongated streamers which are horizontal in the outboard midplane and tilt as they stretch along the sheared magnetic field lines. For such modes, we have

$$k_\perp^2 = k_y^2\,(1 + \hat{s}^2\theta^2), \tag{3}$$

where θ is an extended, angle-like coordinate in the field-line direction. Here, it is implied that the normalized pressure gradient, α, vanishes. Points in the outboard midplane are characterized by $\theta/\pi = \ldots, -4, -2, 0, 2, 4, \ldots$, whereas points in the inboard midplane have $\theta/\pi = \ldots, -3, -1, 1, 3, \ldots$. In practice, the structure of linear toroidal modes can be extended greatly in the θ direction. This suggests the definition of an average value of $k_\perp^2$ according to

$$\langle k_\perp^2\rangle = k_y^2\,(1 + \hat{s}^2\langle\theta^2\rangle), \tag{4}$$

where

$$\langle\theta^2\rangle \equiv \frac{\int \theta^2\,|\phi_{k_y}(\theta)|^2\,\mathrm{d}\theta}{\int |\phi_{k_y}(\theta)|^2\,\mathrm{d}\theta}. \tag{5}$$

The weighting is done in terms of the complex-valued eigenfunction $\phi_{k_y}(\theta)$ for a given set of plasma parameters and a given value of k_y. (For the evaluation of equation (5), the integration boundaries are taken to be -3π and 3π in the present work. We find that choosing a larger integration domain does not substantially alter the results.) Consequently, holding all plasma parameters fixed, $\gamma/\langle k_\perp^2\rangle$ is a function of k_y. An example is shown in figure 3. Here, the physical parameters are: $R/L_n = 3$, $R/L_{T_e} = 6$, $R/L_{T_i} = 0$, $T_e/T_i = 3$, $q = 1.4$, $\hat{s} = 0.8$, $\alpha = 0$, $\epsilon \equiv r/R = 0.16$, $\beta_e \equiv 4\pi n_e T_e/B^2 = 10^{-3}$, $m_i/m_e = 1836$. The plasma consists of electrons and protons, and collisions are neglected. Under these conditions, the relevant microinstabilities are collisionless trapped electron modes, and $\gamma/\langle k_\perp^2\rangle$ peaks around $k_y\rho_s \sim 0.12$, exhibiting a fast (slow) fall-off at low (high) k_y. Interestingly, this behaviour is in qualitative agreement with the electron heat flux spectrum obtained by nonlinear gyrokinetic simulations with the gene code. The respective curve is also shown in figure 3. This is not a coincidence. In fact, one finds that the above method of estimating the relevant k_y range for turbulent transport works quite well in a large region of parameter space. (For more examples, see [10].) In general, the function $\gamma/\langle k_\perp^2\rangle$ tends to have its maximum around $k_y\rho_s \sim 0.1$–0.15, whereas γ/k_y^2 typically peaks at $k_y\rho_s \ll 0.05$. The latter values are, of course, unrealistically small. Thus we find that the averaging procedure (equation (5)) is a crucial aspect of our model.

Now that we have shown the relevance of linear cross-phases and found a reasonably simple way to estimate the transport-dominating k_y range, we can capitalize on these findings and build a quasilinear transport model. In the case of trapped electron mode turbulence, the

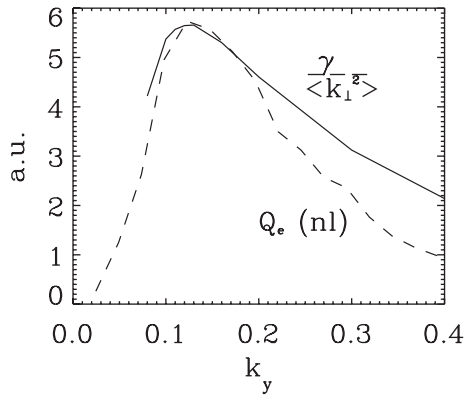

Figure 3. Mixing-length type estimate $\gamma/\langle k_\perp^2\rangle$ as a function of k_y for the parameter set given in the text. The k_y spectrum of the electron heat flux obtained from a nonlinear `gene` simulation is shown for comparison as a dashed line. Here, the $\gamma/\langle k_\perp^2\rangle$ curve has been rescaled to match the nonlinear result at its maximum.

electron heat flux Q_e, the ion heat flux Q_i and the particle flux Γ can be estimated in the following way:

$$\frac{Q_e}{n_e T_e/R} = \mathcal{C} \max_{k_y}\left[\frac{\gamma}{\langle k_\perp^2\rangle}\right]\frac{R}{L_{T_e}}. \tag{6}$$

Here, we used $Q_e = -n_e\chi_e\nabla T_e$. The additional factor of R/L_{T_e} mediates between χ_e and Q_e, and the free dimensionless parameter $\mathcal{C}$ is determined such that Q_e agrees with the nonlinear simulation result for a set of base case parameters. Estimates for Q_i and Γ may be derived from equation (6) via the quasilinear ratios of Q_i/Q_e and Γ/Q_e for the k_y value at which $\gamma/\langle k_\perp^2\rangle$ peaks. In the case of ion temperature gradient driven turbulence, the roles of Q_i and Q_e would be interchanged. In a refined version of this model, we have also taken into account the phase shift information for the dominant transport channel. Here, the right-hand side of equation (6) is multiplied by the sine of the cross phase between fluctuations of the electrostatic potential and those of the pressure for a given value of k_y. Sometimes such a refined model yields slightly better results. An Ansatz similar to ours has been used before quite sucessfully by Kotschenreuther *et al* [11]. In the context of ITG turbulence, they observed that $\mathcal{C}$ 'is a much weaker function of parameters than χ itself'. We confirm this statement and find that it seems to have a surprisingly large range of applicability. The key exception is probably ITG turbulence close to the threshold in R/L_{T_i} which tends to be strongly altered (or even suppressed) by zonal flows.

For clarification, it should be pointed out that the validity of such an approach does not imply that we are dealing with a 'low Reynolds number' situation. The k_y spectra of many relevant quantities exhibit power-law tails at high k_y, indicative of cascade dynamics, (approximate) self-similarity and high dimensionality. However, this 'inertial' range is usually separated from the 'drive' range, in which most of the turbulent transport originates. The coupling between these two scale ranges may be compared with the interaction of medium and small spatial scales in hydrodynamic turbulence. The latter is characterized by a dynamical competition between (linear) viscous dissipation and (nonlinear) energy transfer to smaller scales due to decaying vortices. In the context of plasma microturbulence, this view can sometimes be taken up in a mirrored fashion. As has been demonstrated in the case of electron temperature gradient (ETG) turbulence using $\epsilon \equiv r/R = 0$, primary instabilities drive

secondaries, thus transferring energy to other degrees of freedom and saturating (as well as modifying) the linear modes [12,13]. Although the saturation mechanism in collisionless TEM turbulence is still under investigation, it is interesting to note that the mixing length estimate (equation (2)) can be reinterpreted as a balance between primary and secondary instabilities at long wavelengths. Moreover, the fact that the weighting function $|\phi_{k_y}(\theta)|^2$ tends to exhibit long tails in the low k_y limit (this effect co-determines the relevant k_y value) might indeed be linked to changes in the secondary modes, similar to what was observed in [13]. With these somewhat speculative remarks, we conclude the description of our simple transport model and now turn to some interesting applications.

3. Electron thermal transport from TEM turbulence

In a recent paper, we have described the basic characteristics of TEM turbulence in the collisionless limit [10]. The base case set of plasma parameters was chosen such that ITG modes were subdominant (for simplicity we chose $R/L_{T_i} = 0$, so ITG modes were actually absent) and that the TEMs were mainly driven by the electron temperature gradient (due to $R/L_{T_e} = 6$ and $R/L_n = 3$). These conditions seem to be rather typical for a large number of tokamak experiments at low density and with dominant electron heating that have been performed over the past few years (see, e.g. [14]). The main findings of our study were as follows:

- The zonal flow activity is weak. For example, zeroing out all zonal flows in the course of a simulation does not have a significant affect on the transport level. The root-mean-square of the $\boldsymbol{E} \times \boldsymbol{B}$ shearing rate is comparable to the maximum linear growth rate. This means that with respect to zonal flows, TEM turbulence behaves more like short-wavelength electron temperature gradient (ETG) turbulence [15] than like ITG turbulence [16] which often spins up much stronger zonal flows.
- The turbulence tends to form radially elongated structures (streamers) which drift in the electron diamagnetic direction. Although the TEM streamers are less pronounced than their ETG counterparts [3], the eddies are clearly anisotropic. Of course, this is only possible in the presence of relatively weak zonal flow activity.
- These streamers appear to be remnants of linear modes. For example, Fourier transforming pairs of fluctuating quantities in the periodic (quasi-poloidal) y direction and measuring their cross phases as a function of k_y, one finds that in the transport-dominating long-wavelength regime ($k_y \rho_s \sim 0.1$–0.15), the correlations in the fully developed turbulent state are a pretty faithful reflection of the respective linear properties.

In contrast to conventional quasilinear models, the transport model described in section 2.2 is able to reproduce several features observed in the nonlinear simulations. Among them is the superlinear dependence of the electron heat flux on the safety factor q [10]. Here, we would like to concentrate on the dependence on the normalized electron temperature gradient, R/L_{T_e}. While ITG modes are destabilized only if R/L_{T_i} exceeds a certain threshold, the behaviour of TEMs is more complex. Since the latter can be driven both by $R/L_{T_e} > 0$ and by $R/L_n > 0$, they are unstable for any value of R/L_{T_e} if R/L_n exceeds a certain limit which tends to be of the order of 3. Thus, strictly speaking, there is no critical temperature gradient in this regime. It is questionable, however, to which degree the nonlinear system reflects this behaviour. Moreover, some experiments with dominant electron heating suggest that the electron temperature profiles exhibit (at least) a moderate kind of stiffness under rather generic conditions (see, e.g. [17]). This points to the existence of effective thresholds in R/L_{T_e} and calls for a study of the R/L_{T_e} dependence of the TEM-induced electron heat flux. A scan of the nominal plasma parameters

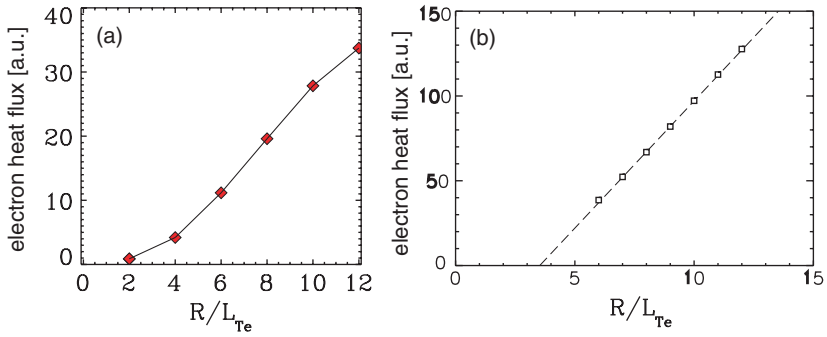

Figure 4. Dependence of TEM-induced electron heat flux on R/L_{T_e} for the nominal parameters mentioned in the text. (*a*) Nonlinear simulation results. (*b*) Results obtained from the transport model described in section 2.2. Both approaches exhibit an offset-linear scaling of the electron heat flux. Moreover, they yield the same effective threshold in R/L_{T_e}.

is shown in figure 4. Although the maximum linear growth rate is always substantial, the electron heat flux exhibits an effective threshold in R/L_{T_e}. Interestingly, the transport model described in section 2.2 can reproduce this behaviour even quanitatively (see figure 4). So both approaches lead us to conclude that even for large values of R/L_n, there is always an effective threshold in R/L_{T_e}.

A second important conclusion from figure 4 is that the dependence of the electron heat flux on R/L_{T_e} is well described by an offset-linear scaling:

$$Q_e \propto \left(\frac{R}{L_{T_e}} - \kappa_c\right) H\left(\frac{R}{L_{T_e}} - \kappa_c\right), \tag{7}$$

where H denotes the Heaviside step function and κ_c is the effective critical gradient. For other sets of plasma parameters, we obtained results which are qualitatively identical. This indicates that the data shown in figure 4 are not a special case but rather prototypical. Expression (7) translates into [18]

$$\chi_e \propto \left(\frac{R/L_{T_e} - \kappa_c}{R/L_{T_e}}\right) H\left(\frac{R}{L_{T_e}} - \kappa_c\right) \tag{8}$$

which is in contrast to the ad hoc Ansatz used in various analyses of the experimental data [14]:

$$\chi_e \propto \left(\frac{R}{L_{T_e}} - \kappa_c\right) H\left(\frac{R}{L_{T_e}} - \kappa_c\right). \tag{9}$$

This suggests that it might be helpful to use equation (8) instead of equation (9) for the analysis of the experimental data. In this context, it is interesting to note that both nonlinear and quasilinear simulations indicate that κ_c exhibits only a weak dependence on most plasma parameters with one main exception, namely magnetic shear. This fact might simplify the use of expression (8) in experimental data analysis somewhat, although the 'stiffness parameter' (prefactor) will still depend strongly on various plasma parameters. Further details will be published elsewhere.

4. Anomalous particle pinch

Another important open question in the area of turbulent transport which can only be addressed adequately in a fully kinetic framework (keeping both ions and electrons, trapped and passing)

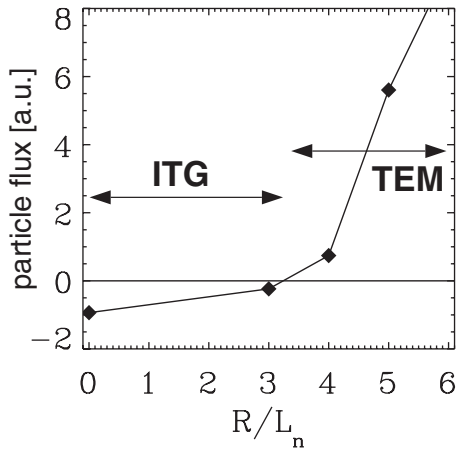

Figure 5. Dependence of the particle flux on R/L_n for the plasma parameters mentioned in the text except for $m_i/m_e = 400$. For $R/L_n \lesssim 3.5$, the turbulence is driven mainly by ITG modes and exhibits a particle pinch. For larger values of R/L_n, the system transitions into a regime which is dominated by density gradient driven TEMs. Here, the particle transport is quite large and outward.

is the existence, nature and role of an anomalous particle pinch. First, we would like to focus on the following scenario which is typical for most present-day (and future) tokamak experiments: $T_e \sim T_i$ and $R/L_{T_e} \sim R/L_{T_i} \gtrsim 6$. For concreteness, we choose $T_e/T_i = 1$, $R/L_{T_i} = R/L_{T_e} = 9$, $q = 1.4$, $\hat{s} = 0.8$, $\alpha = 0$, $\epsilon \equiv r/R = 0.16$, $m_i/m_e = 1836$ and $\beta_e = 10^{-4}$ as our base case values. Collisions are neglected. A linear microinstability analysis reveals that for such plasma parameters and small R/L_n, the turbulence tends to be mainly driven by ITG modes. However, increasing R/L_n, we find that the system transitions into a regime which is instead dominated by density gradient driven TEMs. Here, the particle transport is quite large and outward. For illustration, a R/L_n scan is shown in figure 5. The fact that for small R/L_n, we have $Q_i \gg Q_e$ while for larger R/L_n, we have $Q_i \sim Q_e$, may be taken as another signature of the regime transition from ITG drive to TEM drive.

From an experimental point of view, the value of R/L_n for which the particle flux vanishes is of particular interest. Provided that the particle source in the plasma core is negligible, it is reasonable to expect that fusion plasmas tend to self-organize into states of marginal particle transport. We thus performed a large number of nonlinear `gene` runs to identify the critical R/L_n as a function of the magnetic shear. The result is shown in figure 6. Here, $\hat{s}$ has been varied between 0.4 and 1.2, and one finds a substantial increase of the critical R/L_n with increasing $\hat{s}$. For comparison, we also computed the corresponding results from (*a*) the new quasilinear model described in section 2.2, (*b*) the widely used quasilinear GLF23 model [19] (in the collisionless limit) which is based on gyrofluid equations and (*c*) the turbulent equipartition (TEP) theory by Isichenko and co-workers as described in [20]. While the new quasilinear model agrees with the nonlinear results quite nicely, the other two models are only able to capture the general trend. In the case of GLF23, one source of the observed discrepancy is, of course, the difference in the basic equations. But as it turns out, there is yet another, quite subtle point which can also alter the results quite significantly and which is usually overlooked. In figure 7, the linear phase shifts between the density fluctuations and the electrostatic potential fluctuations are shown as a function of k_y for several values of R/L_n. Negative values correspond to inward particle transport and vice versa. Obviously, for

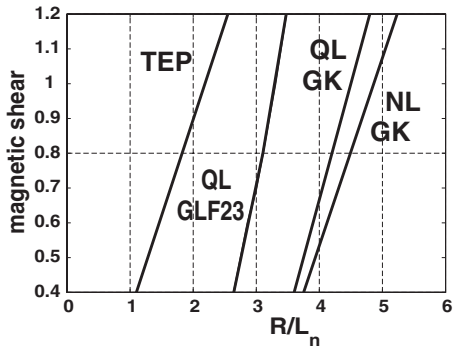

Figure 6. Lines of zero particle flux in the R/L_n-$\hat{s}$ plane for four different models: (*a*) nonlinear gyrokinetic runs with `gene` (NL GK), (*b*) the quasilinear gyrokinetic model described in section 2.2 (QL GK), (*c*) the quasilinear gyrofluid model GLF23 (QL GLF23) and (*d*) TEP.

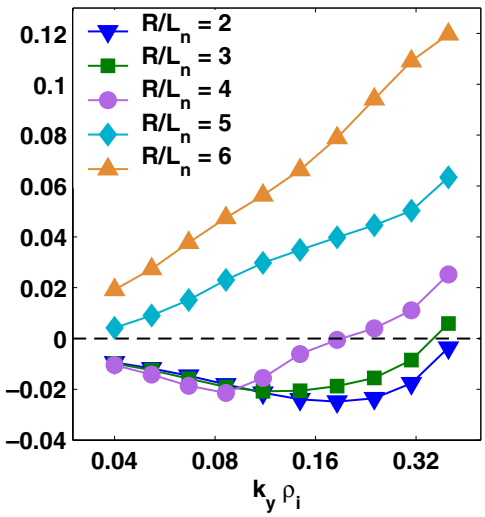

Figure 7. Linear gyrokinetic simulations with the `gs2` code [5]: phase shifts between the density fluctuations and the electrostatic potential fluctuations are shown as a function of k_y for several values of R/L_n. Negative values correspond to inward particle transport and vice versa.

$R/L_n \lesssim 4$ the k_y curves change sign. While for long wavelengths, the quasilinear transport is inwards, for shorter wavelengths the opposite is true. In other words, if the transition point is computed by means of a quasilinear model, the answer will depend on the value of k_y that is chosen. Many authors tend to pick a k_y near the position of the maximum linear growth rate. However, models based on this choice will underestimate the critical R/L_n. As was shown and discussed already in section 2, the nonlinear transport spectra typically peak at much smaller values of k_y and move around as the plasma parameters are changed. Since our modified transport model accounts for these effects, it is able to reproduce the nonlinear results quite nicely. On the other hand, even gyrokinetic models will deviate much more as long as the k_y values are chosen to be too large and parameter independent.

Next, we would like to investigate the role of trapped and passing electrons in pinch physics. Usually, it is assumed that the passing electrons may be taken to be adiabatic

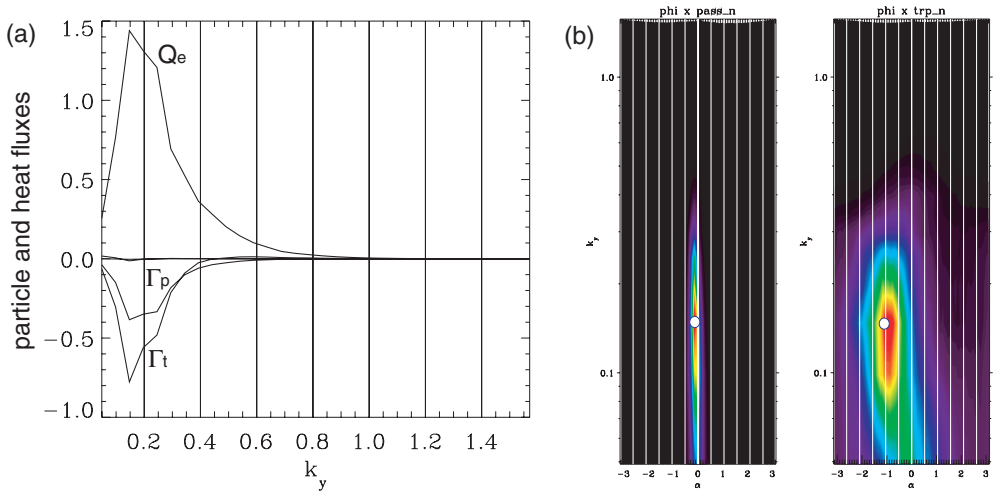

Figure 8. ITG turbulence: (*a*) k_y spectrum of electron heat flux (Q_e) and particle flux carried by trapped/passing electrons (Γ_t and Γ_p). (*b*) Cross phase relations between the electrostatic potential and the trapped/passing electron densities as a function of k_y. The light dots represent the respective linear cross phases at $k_y = 0.15$.

due to their fast parallel motion. If this were true, their contribution to the total particle transport could be neglected, and it would probably suffice to retain only (bounce-averaged) trapped electrons in most two-species core turbulence computations. However, analysing our ITG turbulence simulations, we find that in some cases, a substantial fraction of the particle pinch is actually carried by the passing electrons. An example, using the above parameters (except for $R/L_{T_e} = 12$) and $R/L_n = 1.5$, is shown in figure 8. Although most of the inward particle transport is carried by trapped electrons, the contribution of the passing ones is significant. Inspecting the nonlinear cross phase relations between the electrostatic potential and the trapped/passing electron densities, one finds that they are again quite similar to their respective linear values. In particular, all phase shifts are negative, thus explaining the inward fluxes of both trapped and passing electrons. In the latter case, the adiabaticity breaking is sufficiently large to yield this surprising result. Obviously, this passing electron pinch is basically a quasilinear effect.

Changing the plasma parameters only slightly using $R/L_{T_i} = 7$ instead of $R/L_{T_i} = 9$, the dominant turbulence drive is now a TEM. In this case, we obtain the results displayed in figure 9. While the trapped electrons lead to a net particle transport which is directed outwards, the passing electrons induce a particle pinch which overcompensates the trapped electron contribution. Thus, TEM turbulence is able to produce a particle pinch which is carried solely by passing electrons. (A similar result has been obtained by Dorland and Hallatschek [21]). As can be inferred from figure 9, this is again a quasilinear effect, like in the ITG case. Although the TEM scenario 'trapped electrons move outwards and passing electrons move inwards' seems to hold quite generically, our simulations show that R/L_{T_i} needs to exceed a certain nonuniversal threshold in order for the total particle flux to become negative (compare the results for $R/L_{T_i} = 0$ presented in [10]). Finally, we would like to present an argument which is based on the results presented in [10] and which explains why in TEM turbulence driven by electron temperature gradients, the particle transport carried by trapped electrons is expected to be outwards. The electron heat flux in such a situation is mainly due to fluctuations of the *perpendicular* electron temperature. The latter are, in turn,

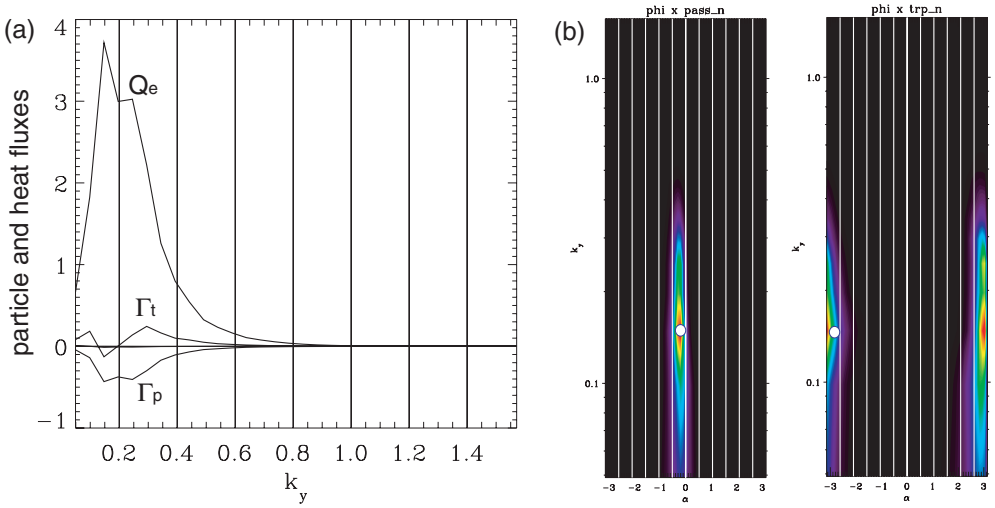

Figure 9. Same as figure 8 but for TEM turbulence.

well correlated with the density fluctuations of trapped electrons since both quantities are dominated by regions in velocity space with a relatively large perpendicular component. Thus the particle flux induced by trapped electrons will tend to follow the electron heat flux which is clearly outwards. This leaves as the only option for a TEM particle pinch a situation like the one described above: passing electrons move inwards, overcompensating the outward flux of trapped electrons. Such a TEM-driven particle pinch seems to be most relevant to experiments with $T_e \gg T_i$ and/or $R/L_{T_e} \gg R/L_{T_i}$. Under these conditions, TEMs are more unstable than ITG modes.

Finally, we would like to point out that several studies have shown a strong dependence of the ITG-induced particle pinch on collisionality [22,23]. In particular, the pinch disappears completely above a critical value of collisionality. This threshold tends to be quite small so that most present-day (and future) experiments are expected to lie in a regime which does not exhibit an ITG pinch [24]. This finding raises many questions, of course, some of which will be addressed in future publications.

5. Summary

In summary, we have used nonlinear and quasilinear gyrokinetics in tandem to explore two different sets of questions in the general area of turbulent transport in fusion plasmas. First, we found that the TEM-induced electron heat flux exhibits a superlinear scaling with the safety factor q and an offset-linear scaling with the normalized electron temperature gradient R/L_{T_e}. Both results are in good agreement with experimental observations but cannot be obtained in the framework of conventional quasilinear models. Second, we showed that an anomalous particle pinch exists both in ITG-dominated and in TEM-dominated systems. In both cases, it is important to retain nonadiabatic passing electrons. In the ITG case, the pinch is carried mainly by trapped electrons, but passing electrons may also contribute in a significant way. And in the TEM case, a particle pinch exists if and only if the inward flux of passing electrons is able to overcompensate the outward flux of trapped electrons. This is typically the case if R/L_{T_i} exceeds a certain nonuniversal threshold.

Acknowledgments

We gratefully acknowledge helpful discussions with A G Peeters and F Ryter.

References

[1] Frieman E A and Chen L 1982 *Phys. Fluids* **25** 502
[2] Brizard A 1989 *J. Plasma Phys.* **41** 541
[3] Jenko F, Dorland W, Kotschenreuther M and Rogers B N 2000 *Phys. Plasmas* **7** 1904
[4] Dannert T and Jenko F 2004 *Comput. Phys. Commun.* **163** 67
[5] Kotschenreuther M, Rewoldt G and Tang W M 1995 *Comput. Phys. Commun.* **88** 128
[6] Dannert T 2005 *PhD Thesis* TU, München http://tumb1.biblio/tu-muenchen.de/publ/diss/ph/2005/dannert.pdf
[7] Rosenbluth M N and Hinton F L 1998 *Phys. Rev. Lett.* **80** 724
[8] Hinton F L and Rosenbluth M N 1999 *Plasma Phys. Control. Fusion* **41** A653
[9] Candy J, Waltz R E and Dorland W 2004 *Phys. Plasmas* **11** L25
[10] Dannert T and Jenko F 2005 *Phys. Plasmas* **12** 072309
[11] Kotschenreuther M, Dorland W, Beer M A and Hammett G W 1995 *Phys. Plasmas* **2** 2381
[12] Cowley S C, Kulsrud R M and Sudan R 1991 *Phys. Fluids* B **3** 2767
[13] Jenko F and Dorland W 2002 *Phys. Rev. Lett.* **89** 225001
[14] Garbet X *et al* 2004 *Plasma Phys. Control. Fusion* **46** 1351
Garbet X *et al* 2005 *Plasma Phys. Control. Fusion* **47** 957
[15] Jenko F and Kendl A 2002 *Phys. Plasmas* **9** 4103
[16] Hahm T S, Beer M A, Lin Z, Hammett G W, Lee W W and Tang W M 1999 *Phys. Plasmas* **6** 922
[17] Ryter F *et al* 2001 *Phys. Rev. Lett.* **86** 2325
[18] Peeters A, Angioni C, Apostoliceanu M, Jenko F, Ryter F and the ASDEX Upgrade Team 2005 *Phys. Plasmas* **12** 022505
[19] Waltz R E, Staebler G M, Dorland W, Hammett G W, Kotschenreuther M and Konings J A 1997 *Phys. Plasmas* **4** 2482
[20] Isichenko M B, Gruzinov A V and Diamond P H 1995 *Phys. Rev. Lett.* **74** 4436
[21] Hallatschek K and Dorland W 2005 *Phys. Rev. Lett.* **95** 055002
[22] Angioni C, Peeters A G, Pereverzev G V, Ryter F and Tardini G 2003 *Phys. Rev. Lett.* **90** 205003
[23] Estrada-Mila C, Candy J and Waltz R E 2005 *Phys. Plasmas* **12** 022305
[24] Angioni C *et al* 2005 Collisionality dependence of density peaking in quasi-linear gyrokinetic calculations *Phys. Plasmas*